Supporting Information

Multiheme Cytochrome Mediated Redox Conduction Through *Shewanella oneidensis* MR-1 Cells

Shuai Xu,[†] Alexandre Barrozo,[‡] Leonard M. Tender[‖], Anna I. Krylov,[‡] and Mohamed Y. El-Naggar[*†‡§]

† Department of Physics and Astronomy, University of Southern California, Los Angeles, California 90089, United States

‡ Department of Chemistry, University of Southern California, Los Angeles, California 90089, United States

‖ Center for Bio/Molecular Science and Engineering, Naval Research Laboratory, Washington, D.C. 20375, United States

§ Department of Biological Sciences, University of Southern California, Los Angeles, California 91030, United States

Experimental Methodology

Cultivation

Shewanella oneidensis MR-1 culture was initiated by inoculating cells directly from a frozen (-80 ˚C) stock into LB broth and incubated at 30 °C till an optical density (OD_{600} measured at a wavelength of 600nm) of 2.4-2.6 was measured. From this pre-culture, 2 mL was pelleted by centrifugation at 4226 × g for 5 min, washed three times, and re-suspended in 100 mL of defined medium for a subsequent anaerobic growth. The defined medium contains 50mM PIPES, 28 mM NH_4Cl, 1.3 mM KCl, 4.3 mM $NaH_2PO_4 \cdot H_2O$, 20 mM sodium DL-lactate as the electron donor, and 18 mM sodium fumarate as the electron acceptor. In addition, amino acids and trace minerals stock solutions were used to supplement the medium as described previously.[1-2] The pH of the medium was adjusted to 7.1 with NaOH. Cells were grown at 30 °C in the defined medium up to an OD_{600} of 0.15 before transfer to the bioelectrochemical reactor.

Electrochemical Setup

All electrochemical experiments were performed in a 100 mL bioreactor placed in an anaerobic chamber (Bactron 300, *Sheldon Manufacturing, Inc.* Cornelius, OR) filled with 95% N_2 and 5% H_2. Reactors contained an Ag/AgCl reference electrode (1M KCl, *CH Instruments*, Austin, TX) and a platinum wire counter electrode (*Sigma*, St. Louis, MO). Indium tin oxide (ITO) patterned Interdigitated Array (IDA) electrodes (IDA Model#012128, *ALS Co., Ltd*, Japan) were utilized as the working electrodes (source and drain) for the *in situ* conduction measurements. The IDA electrodes consist of 65 pairs of parallel ITO "electrode arms" (each arm is 2 mm long × 10 μm wide × 100 nm thick). Each adjacent arm is electrically connected to opposite ends of the array, forming two separated but interdigitated electrodes (electron source and drain). IDAs were used as received except for gentle washing with deionized water. Coated copper wires were affixed to the each working electrode at the terminal contact pads using silver paint (*SPI Supplies*, West Chester, PA). These connections were then sealed with epoxy (*Gorilla Glue*, Cincinnati, OH).

Electrochemical Measurements

The anaerobically pre-grown *Shewanella oneidensis* MR-1 culture was transferred to the IDA-containing bioreactor in the anaerobic chamber to maintain anoxic conditions. Both IDA electrodes were poised at 0.44 (vs. SHE) overnight. This resulted in an increase in catalytic current over time at both electrodes due to the electrode-attached cells coupling the oxidation of lactate with EET to the electrode surface. Biomass coverage over the electrodes was determined *ex situ* by both fluorescent microscopy (Nikon Eclipse Ti-E) and atomic force microscopy (Asylum Cypher ES).

The bipotentiostat consisted of two Gamry Reference 600 potentiostats connected with a communication cable and used in a MultEchem configuration (*Gamry*, Warminster, PA). Electrochemical gating as accomplished using a Linked Cyclic Voltammetry script provided by the manufacturer. After the electrochemical cultivation step, the bioreactor supernatant was carefully replaced with fresh defined medium containing 20 mM lactate and no fumarate to remove planktonic cells, the presence of which was found to result in higher noise (likely due to cells transiently contacting the electrodes) and to ensure that conduction is occurring through the

electrode-attached cells. After a short period of amperometry (at 0.44 V, vs. SHE) to establish equilibrium between the new electrochemical environment and the IDA-attached cells, electrochemical gating measurements were performed using the bipotentiostat. Gating measurements were performed by simultaneously scanning the potentials of the source (E_S) and drain (E_D) electrodes at the same scan rate (ν = 1 mV s^{-1}), while maintaining a constant potential offset ($V_{SD} = E_D - E_S$ = 0.02 V) and measuring the source and drain currents separately at each electrode.

Electrochemical gating experiments were performed under both turnover condition (lactate present) and non-turnover condition (lacking lactate). After turnover gating measurements, the reactor supernatant was carefully replaced with fresh defined medium (no electron donor or acceptor), in order to transition to non-turnover condition. A constant potential of 0.44 V was applied at both source and drain electrodes to exhaust any residue lactate in the reactor. After 24 hours of transition, the amperometric current gradually decreased to almost zero, which signaled the establishment of the non-turnover condition, after which gating measurements were performed.

When performing gating experiments, the observed total current at each electrode (for a given potential) can be generally expressed as $I = I_{cat} + I_{redox} \pm I_{cond}$. The first term, I_{cat}, is due to cellular catalytic oxidation of lactate and is zero under the lactate-free (non-turnover) conditions under which we performed the gating measurements. The second term, I_{redox}, is due to the intrinsic redox activity of the electrode-accessible cellular cofactors i.e. Faradaic charging/discharging of redox cofactors in response to gate potential. The final term, I_{cond} (equal in magnitude but opposite in sign at the drain vs. source electrode), is the V_{SD}-driven source-to-drain conduction current.[3-4] It is important to note that I_{redox} is therefore a background contribution that is expected to contribute to a current peak if not subtracted out from the total current to arrive at the desired conduction current, I_{cond}. Here we used two different methods to perform this background subtraction and cross-checked them against each other. For small enough V_{SD}, the background currents (I_{redox}) are expected to be equal at the source and drain electrodes. In the first method, therefore, subtracting raw source current from raw drain current at each gate potential therefore yields $2I_{cond}$. To check the accuracy of this approach under our experimental conditions (i.e. small I_{redox} difference between the two electrodes for V_{SD} = 0.02 V, relative to I_{cond}), we cross-checked the resulting I_{cond} against a second background subtraction method,[3] where separate V_{SD} = 0 (and therefore I_{cond} = 0) scans, one each for the respective potential ranges of the source and drain electrodes e.g. -600 to 300 and -580 to 320 mV, are performed to independently measure the background current. The latter background current at each electrode and potential is subtracted from current measured at each electrode for V_{SD} = 0.02 V at each potential. This second method of background subtraction yields I_{cond} at each electrode, with opposite signs to account for electron current exiting and entering the source and drain electrodes, respectively. Figure S2 shows that the measured I_{cond} was indeed consistent for both background-subtraction methods. For this reason, the simpler procedure (i.e. without a separate V_{SD} = 0 scan) was used for the temperature-dependent measurements as it was both less tedious and resulted in lower noise measurements (likely due to the possibility of a change in cellular activity in the time required to perform two full scans).

Temperature-dependent Measurements

Temperature-dependent gating measurements were performed under non-turnover condition, by placing the bioreactor in a water bath (*VWR*, Radnor, PA) with precise temperature control in the

anaerobic chamber. The IDA temperature was stepped from 38 °C to 25 °C in approximately 2 °C increments. The same bioreactor was also placed in an ice bath (~4 °C measured IDA temperature) to extend the temperature range of the gating measurements. Each gating measurement was performed only after the thermometer indicated a stable temperature (~15 min). The thermal activation energy (E_a) was determined by fitting the experimental data to $I_{cond} = V_{SD}\frac{A}{T}e^{-\frac{E_a}{kT}}$ using the least squared deviation method. Measurements were performed on three independent biological replicates, in order to estimate the uncertainty in the activation energy E_a = 0.29±0.03 eV.

Computational Methodology

Kinetic Monte Carlo model

We use a Kinetic Monte Carlo algorithm to stochastically sample how electrons are transported across complex networks. Such models were previously used to study conductance across MtrF,[5] offering insight on the nature of electron occupancy and flow through the many hemes of the system. We adopted the same scheme as used in Ref. [5], which is nearly identical for MtrC and MtrF, changing only the individual step-wise electron transfer rates between hemes. The ten distinct redox sites are arranged as shown in Fig. S6. Each site can be either oxidized or reduced (with or without a transported electron). Electrons can be transferred between adjacent sites with a probability proportional to the rate of electron transfer between the sites. Such rates were estimated theoretically.[6] They can also be inserted into an entrance heme or ejected from an exit heme. Hemes 2, 5, 7 and 10 were chosen to be electron gateways, and simulations were performed along the following bidirectional routes: 10↔5, 2↔7, and 10↔7. Ingress and egress of electrons is also proportional to a rate (10^8 s^{-1}), which we defined to be the highest among all the step-wise electron transfer rates, to make sure these processes would not limit transport through the protein's decaheme chain at any moment.

Monte Carlo simulations rely on stochastic sampling. The stochastic events taking place are whether an electron is being inserted into the system, moving between sites, exiting the system, or none of the above. Information on the process of choice of stochastic events was described previously.[5] For the 10↔5 route, we performed simulations for MtrC and MtrF considering step-wise heme-to-heme transfer rates from the two distinct electron conductance regimes described in detail in Ref. [6]: electron hopping with heme 7 either available for electron transfer (one-electron) or always reduced (referred to as the two-electron case). These scenarios were used to calculate the free energy landscape of the protein, and corresponding set of step-wise heme-to-heme rates.[6] In the KMC simulations, however, the system was not constrained to have only a single electron at a time, and multiple sites could be reduced at once.[5] We performed simulations for temperatures between 286.15 and 306.15 K, with 2 K intervals (a total of 11 different temperatures). For a given protein, temperature and *i*↔*j* route, we considered the transport from heme *i* to heme *j*, and *vice versa*, counting how many electrons would exit the system as our electron flow over the simulation time. Each simulation consisted of 10^9 steps, and we performed sets of four independent simulations, averaging the results. This number was sufficient for convergence of our results, with asymptotic standard error of less than 5%. From these temperature-dependent simulations, the activation barrier (E_a) was obtained with the same fitting procedure as the experimental measurements (Equation 1 in main text).

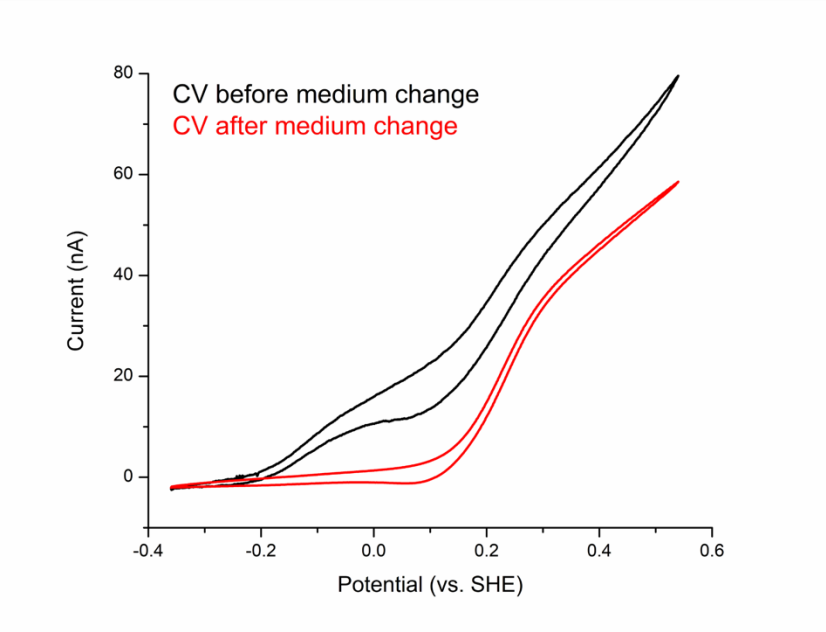

Figure S1. Cyclic voltammetry (CV) of *S. oneidensis* MR-1 on indium tin oxide interdigitated electrode arrays, before and after medium change. Two redox pathways are observed, consistent with previous reports of extracellular electron transfer in *S. oneidensis*; a flavin-dependent pathway at -0.23 V onset potential, and a cytochrome-mediated pathway at 0.17 V onset potential. Only the latter is retained after medium exchange as a result of removal of flavins.

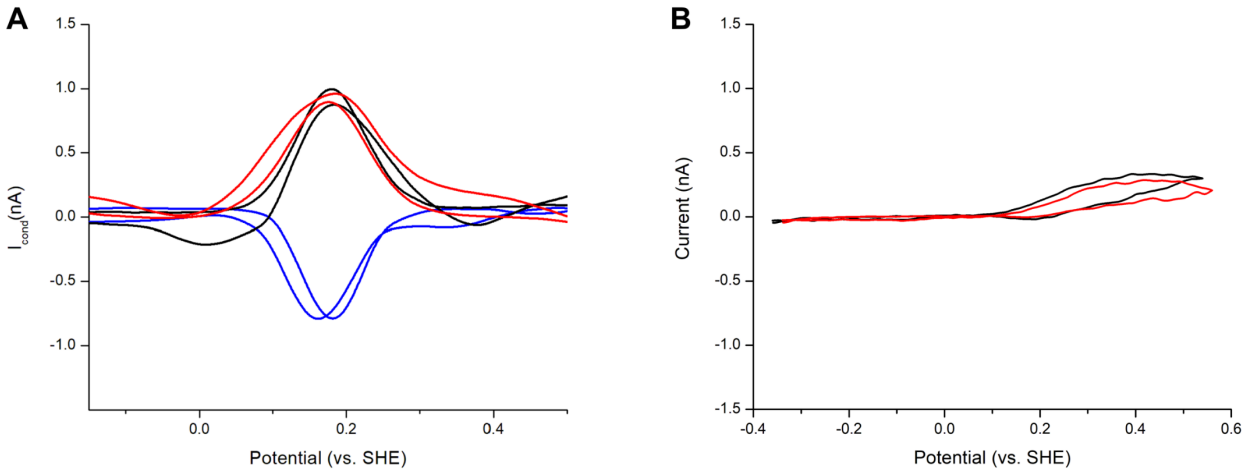

Figure S2. (A) A comparison of conduction current I_{cond} obtained using the two different background subtraction methods applied to the electrochemical gating measurements of wild-type *S. oneidensis* MR-1. Red: by subtracting raw source current from raw drain current in the non-turnover gating V_{SD}=0.02 V scan (e.g. Figure 2) to yield $2I_{cond}$ (I_{cond} plotted against gate potential $E_G=(E_S+E_D)/2$). Black and blue: by subtracting the measured background current obtained by separate V_{SD}=0 scans from the current observed in the V_{SD}=0.02 V scan at each electrode and each potential, to yield I_{cond} at the drain and source electrodes, respectively (plotted against their respective potentials on source/drain electrodes). Opposite signs account for electron current exiting and entering the source and drain electrodes, respectively. The measured I_{cond} is consistent for both background-subtraction methods. (B) Results of a control using two large split electrodes separated by a 1 mm gap too large to be bridged by cells; no peak in conduction is observed and same sign current observed at the source (black) and drain (red) electrodes indicate leftover background, rather than conduction, currents.

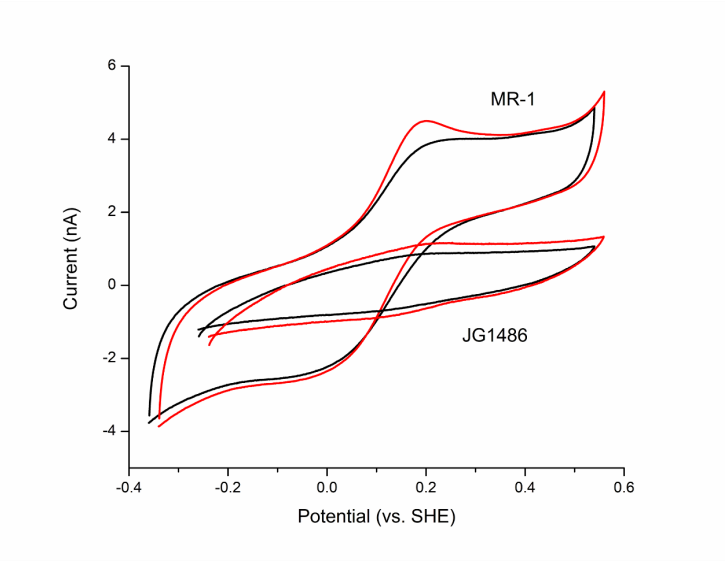

Figure S3. Cyclic voltammetry from gating experiments of wild-type *S. oneidensis* and the JG1486 mutant lacking eight functional periplasmic and outer-membrane cytochromes (Δ*mtrB*/Δ*mtrE*/Δ*mtrC*/Δ*omcA*/Δ*mtrF* /Δ*mtrA*/Δ*mtrD*/Δ*dmsE*/Δ*SO4360*/Δ*cctA*/Δ*recA*), confirming the assignment of the redox peaks to cytochromes.

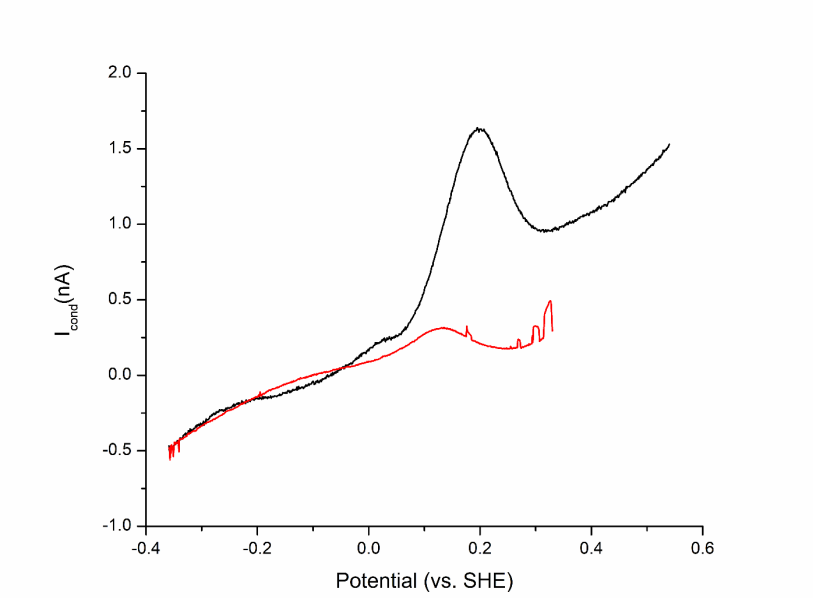

Figure S4. Comparison of a cell-covered IDA and a sterile IDA exposed to the spent medium from the same cells. Dependence of conduction current I_{cond} on gate potential E_G for cellular conduction (black) vs. spent medium (red) contribution.

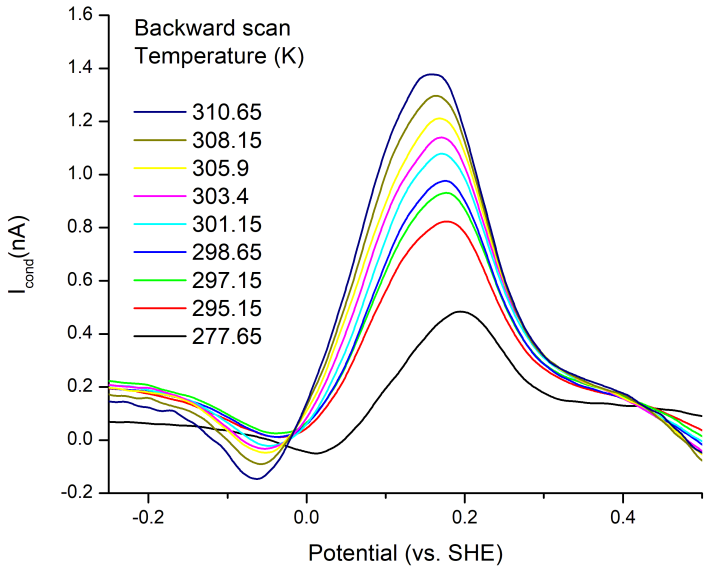

Figure S5. Dependence of conduction current I_{cond} on gate potential E_G for different temperatures (backward scans from the same experiment as Figure 3A showing the forward scan results).

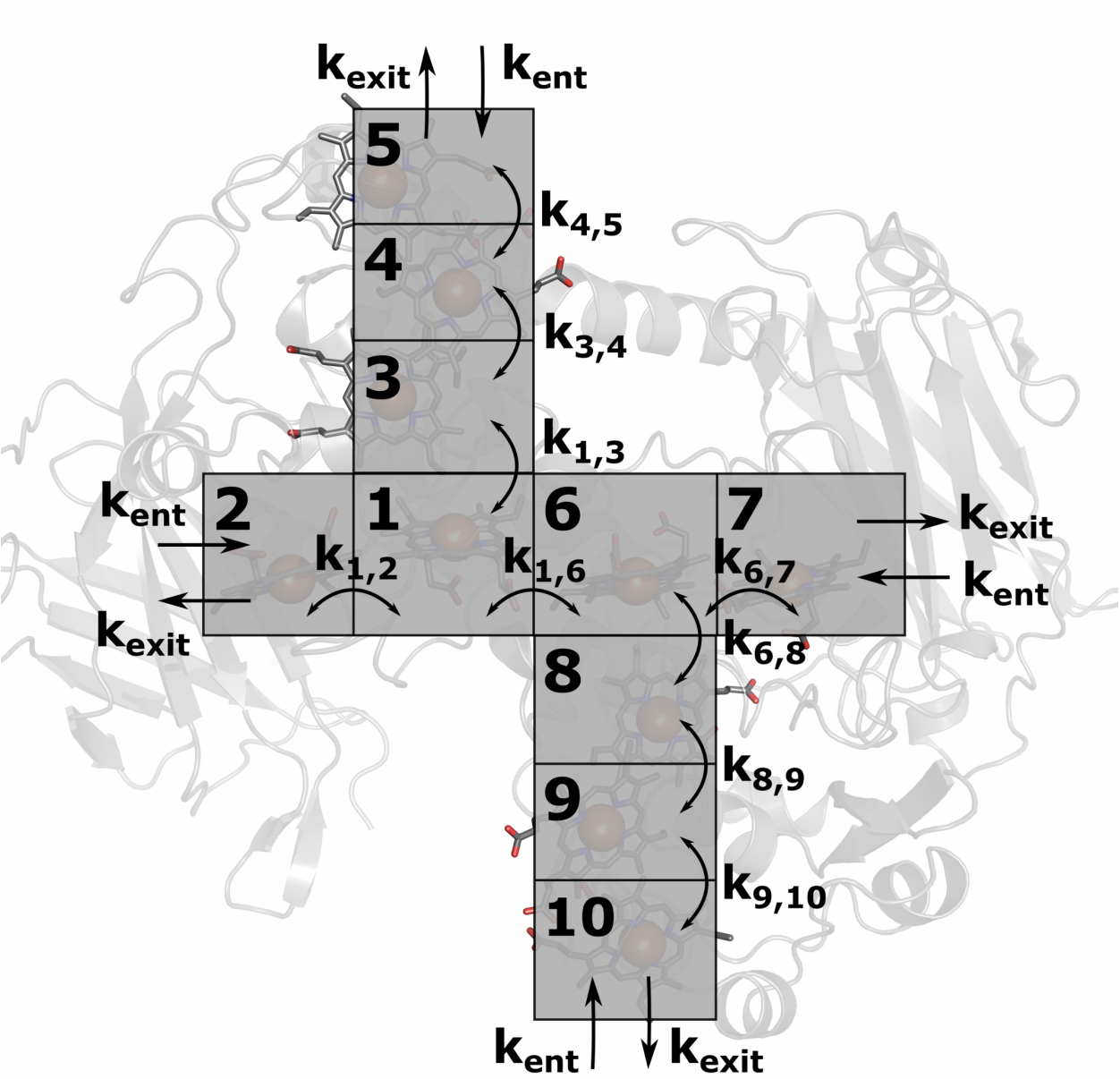

Figure S6. A scheme illustrating the KMC model in MtrC. The representation is the same for MtrF. Hemes 2, 5, 7, and 10 are the gateways for electron injection to and ejection from the system. Electron transfer is only allowed between adjacent hemes when the donor site is reduced, and the acceptor site is oxidized. The KMC model is described in detail in Ref [5] and the step-wise heme-to-heme rates are detailed in Ref [6]. Numbering convention of the hemes is the same as those in the crystal structures (MtrC PDB: 4LM8 and MtrF PDB: 3PMQ) and literature.

References

1. Bretschger, O.; Obraztsova, A.; Sturm, C. A.; Chang, I. S.; Gorby, Y. A.; Reed, S. B.; Culley, D. E.; Reardon, C. L.; Barua, S.; Romine, M. F.; Zhou, J.; Beliaev, A. S.; Bouhenni, R.; Saffarini, D.; Mansfeld, F.; Kim, B. H.; Fredrickson, J. K.; Nealson, K. H., Current production and metal oxide reduction by Shewanella oneidensis MR-1 wild type and mutants. *Appl Environ Microb* **2007,** *73* (21), 7003-7012.
2. Prakash, G. K. S.; Viva, F. A.; Bretschger, O.; Yang, B.; El-Naggar, M.; Nealson, K., Inoculation procedures and characterization of membrane electrode assemblies for microbial fuel cells. *Journal of Power Sources* **2010,** *195* (1), 111-117.
3. Yates, M. D.; Golden, J. P.; Roy, J.; Strycharz-Glaven, S. M.; Tsoi, S.; Erickson, J. S.; El-Naggar, M. Y.; Barton, S. C.; Tender, L. M., Thermally activated long range electron transport in living biofilms. *Phys Chem Chem Phys* **2015,** *17* (48), 32564-32570.
4. Yates, M. D.; Strycharz-Glaven, S. M.; Golden, J. P.; Roy, J.; Tsoi, S.; Erickson, J. S.; El-Naggar, M. Y.; Barton, S. C.; Tender, L. M., Measuring conductivity of living Geobacter sulfurreducens biofilms. *Nat Nanotechnol* **2016,** *11* (11), 910-913.
5. Byun, H. S.; Pirbadian, S.; Nakano, A.; Shi, L.; El-Naggar, M. Y., Kinetic Monte Carlo Simulations and Molecular Conductance Measurements of the Bacterial Decaheme Cytochrome MtrF. *Chemelectrochem* **2014,** *1* (11), 1932-1939.
6. Barrozo, A.; El‐Naggar Mohamed, Y.; Krylov Anna, I., Distinct Electron Conductance Regimes in Bacterial Decaheme Cytochromes. *Angewandte Chemie International Edition* **2018,** *57* (23), 6805-6809